MDPI

Article

Hydrogeochemical Insights into the Sustainable Prospects of Groundwater Resources in an Alpine Irrigation Area on Tibetan Plateau

Shaokang Yang [1,2,3], Zhen Zhao [1,2,3,*], Shengbin Wang [1,2,3], Shanhu Xiao [1,2,3], Yong Xiao [4,5,6,*], Jie Wang [4,7], Jianhui Wang [1,2,3], Youjin Yuan [1,2,3], Ruishou Ba [1,2,3], Ning Wang [8], Yuqing Zhang [4,7], Liwei Wang [4,7] and Hongjie Yang [4,7]

[1] Bureau of Qinghai Environmental Geological Prospecting, Xi'ning 810007, China
[2] Key Lab of Geo-Environment of Qinghai Province, Xi'ning 810007, China
[3] Qinghai 906 Engineering Survey and Design Institute Co., Ltd., Xi'ning 810007, China
[4] Faculty of Geosciences and Engineering, Southwest Jiaotong University, Chengdu 611756, China
[5] Fujian Provincial Key Laboratory of Water Cycling and Eco-Geological Processes, Xiamen 361021, China
[6] MOE Key Laboratory of Groundwater Circulation and Environmental Evolution, China University of Geosciences (Beijing), Beijing 100083, China
[7] Sichuan Province Engineering Technology Research Center of Ecological Mitigation of Geohazards in Tibet Plateau Transportation Corridors, Chengdu 611756, China
[8] School of Water and Environment, Chang'an University, Xi'an 710054, China
* Correspondence: zhaozhen_906@163.com (Z.Z.); xiaoyong@swjtu.edu.cn (Y.X.)

Abstract: The Tibetan Plateau is the "Asia Water Tower" and is pivotal for Asia and the whole world. Groundwater is essential for sustainable development in its alpine regions, yet its chemical quality increasingly limits its usability. The present research examines the hydrochemical characteristics and origins of phreatic groundwater in alpine irrigation areas. The study probes the chemical signatures, quality, and regulatory mechanisms of phreatic groundwater in a representative alpine irrigation area of the Tibetan Plateau. The findings indicate that the phreatic groundwater maintains a slightly alkaline and fresh status, with pH values ranging from 7.07 to 8.06 and Total Dissolved Solids (TDS) between 300.25 and 638.38 mg/L. The hydrochemical composition of phreatic groundwater is mainly HCO_3-Ca type, with a minority of HCO_3-Na·Ca types, closely mirroring the profile of river water. Nitrogen contaminants, including NO_3^-, NO_2^-, and NH_4^+, exhibit considerable concentration fluctuations within the phreatic aquifer. Approximately 9.09% of the sampled groundwaters exceed the NO_2^- threshold of 0.02 mg/L, and 28.57% surpass the NH_4^+ limit of 0.2 mg/L for potable water standards. All sampled groundwaters are below the permissible limit of NO_3^- (50 mg/L). Phreatic groundwater exhibits relatively good potability, as assessed by the entropy-weighted water quality index (EWQI), with 95.24% of groundwaters having an EWQI value below 100. However, the potential health risks associated with elevated NO_3^- levels, rather than NO_2^- and NH_4^+, merit attention when such water is consumed by minors at certain sporadic sampling locations. Phreatic groundwater does not present sodium hazards or soil permeability damage, yet salinity hazards require attention. The hydrochemical makeup of phreatic groundwater is primarily dictated by rock–water interactions, such as silicate weathering and cation exchange reactions, with occasional influences from the dissolution of evaporites and carbonates, as well as reverse cation-exchange processes. While agricultural activities have not caused a notable rise in salinity, they are the main contributors to nitrogen pollution in the study area's phreatic groundwater. Agricultural-derived nitrogen pollutants require vigilant monitoring to avert extensive deterioration of groundwater quality and to ensure the sustainable management of groundwater resources in alpine areas.

Keywords: hydrochemistry; groundwater quality; nitrogen contamination; agricultural pollution; alpine region

1. Introduction

Alpine regions, namely high mountain regions, are of great importance to the whole world as they are the source of water for almost all watersheds [1–3]. It is estimated that about 25% of the world's population will rely on the water resources of alpine regions by 2050 [4,5]. Although water resources are abundant in the world's alpine regions, the majority of water resources are in the form of solid water (such as snow and ice) [6] and are difficult for human society to use directly. The only water resource that is easily accessible to humans is liquid freshwater, including surface water (river and lake water, etc.) [7] and groundwater [8]. Meanwhile, the surface water of rivers and lakes is generally unstable [9] and difficult to use as a sustainable water supply for the human community [10]. Groundwater is the ideal source of water for human society because it is a good buffer against external changes [11–13]. Thus, a deep understanding of the fresh liquid water beneath the ground surface is crucial for a sustainable water supply for human society in alpine regions.

Groundwater availability is constrained by both water quantity and water quality. The alpine region is usually rich in water resources due to abundant precipitation and snow/glacier melt water, especially in the basins or valleys [14]. Thus, water quantity is not the most dominant factor influencing the availability of groundwater in alpine regions. On the contrary, water quality is becoming an increasingly important factor limiting groundwater availability [15]. Naturally, groundwater quality in alpine regions is determined by many geogenic toxic elements (such as fluoride and arsenic) [16,17] or potential high salinity [18,19]. In addition, climate change is the most important global concern in all aspects, including the hydrosphere and related spheres [20–24]. The alpine zone is experiencing significant warming and increased humidity, which directly affects groundwater quality and the hydrological cycle [18,24–27]. The melting of glaciers and the degradation of permafrost have resulted in enhanced weathering and dissolution of minerals within mountainous regions and permafrost layers. Consequently, the hydraulic connectivity among various water bodies has been progressively augmented [28–30]. Numerous studies have demonstrated that the hydrological cycle's mechanisms have become increasingly complex due to these influences, leading to alterations in the hydrochemical characteristics and the patterns of hydrochemical quality within groundwater systems [28,31,32].

Furthermore, amidst rapid socio-economic development and population expansion, human activities have emerged as a significant factor affecting water ecosystems [15]. It has been documented that anthropogenic substances are present in numerous aquifers globally [33–36]. Groundwater contamination by toxic substances is an escalating environmental concern due to their potential detrimental effects on human health and aquatic ecosystems [37–39]. Agricultural and livestock activities in the alpine zone have experienced notable expansion [40]. The excessive application of chemical fertilizers and pesticides, coupled with pollutants from livestock and poultry farming, may pose a significant risk to the chemical integrity of groundwater [41–43]. Considering the dual pressures from dramatic shifts in the natural environment and human activities, it is imperative to focus on the hydrochemical characteristics and their formation mechanisms, as well as the sustainability of groundwater resources in alpine areas.

The Tibetan Plateau, often referred to as the "Asia Water Tower", is a pivotal area for ecological security and water resource management in Asia. As a quintessential alpine region, it exhibits heightened sensitivity to environmental fluctuations [44]. The current study examines the Tongde Basin in the northeastern Tibetan Plateau as a case study to elucidate the hydrochemical formation patterns and the availability of groundwater resources in the basin's eastern sector, an area characterized by relatively intensive agricultural and livestock activities. Specifically, the study aims to (1) delineate the hydrochemical characteristics of groundwater; (2) uncover the mechanisms behind groundwater's hydrochemical formation; and (3) assess the overall water quality of groundwater, including its suitability for sustainable potable and irrigation usages. This research is poised to offer scientific guidance on hydrochemical aspects, thereby enhancing water ecosystem security and

ensuring water use sustainability in the alpine region of the Tibetan Plateau and other similar regions worldwide.

2. Materials and Methods

2.1. Study Area Description

The study area, situated in the central region of the Tongde Basin on the northeastern Tibetan Plateau, is defined by longitudes from 100°43′22.79″ E to 101°5′16.80″ E and latitudes from 35°6′7.21″ N to 35°21′14.43″ N, encompassing an area of 929.46 km² (Figure 1). The topography of the study area is characterized by higher elevations in the southeast and lower elevations in the northwest. The northwestern flank of the study area is typified by a piedmont sloping plain and a valley belt plain, whereas the southeastern side is predominantly composed of tectonically uplifted mid- to high-altitude mountainous terrain. The region's elevation varies between 3219 m and 4057 m above sea level. The hydrological system of the study area is predominantly composed of three rivers. The Baqv River, one of these, courses from east to west across the northern plain. The Cihawuqv River and the Ningxiuqv River, which are tributaries of the Baqv River, originate from the southern mountainous region, flow towards the northern plain, and eventually converge with the Ba River. These rivers bring the surface water of mountainous areas to the plain and recharge aquifers through infiltration in the piedmont. The study area is characterized by a continental plateau climate, with extended winters and abbreviated summers, frequent winds, and scant precipitation. The annual mean temperature fluctuates between −0.77 °C and 1.69 °C, presenting generally low temperatures. Annual precipitation varies between 544 mm and 837 mm, with a mean of 688 mm. Over 80% of the annual rainfall occurs from May through September. This region has a potential evaporation rate of 790 mm, demonstrating a minimal disparity with precipitation.
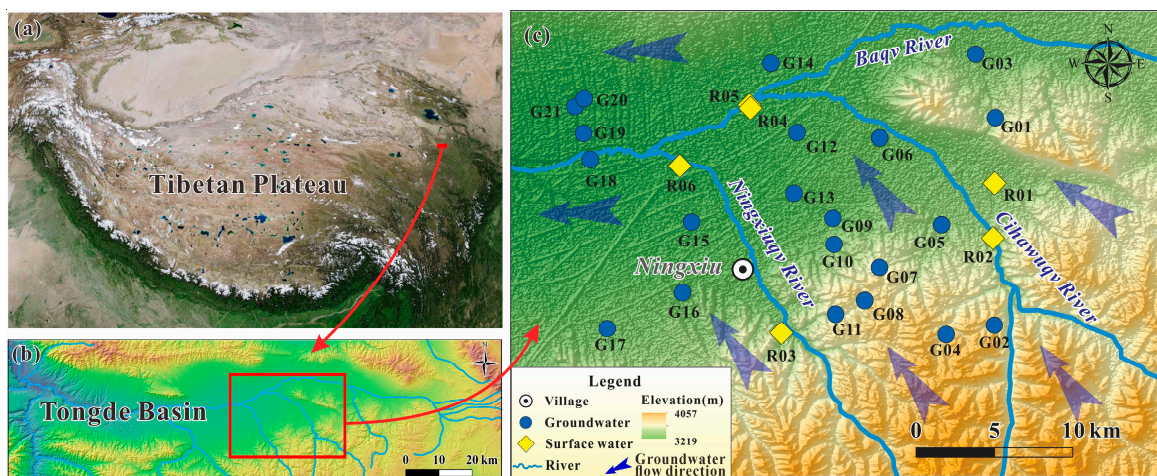

Figure 1. Spatial location of (**a**) the Tongde Basin on the Tibetan Plateau, (**b**) study area in Tongde Basin, and (**c**) the sampling sites of surface water and groundwater.

Geologically, the Quaternary sediments are predominantly found in the piedmont sloping plain and valley belt plain of the northwestern part of the study area. These sediments primarily consist of alluvial deposits and constitute the principal aquifer system within the region. From the southeast to the northwest, the aquifer type transitions from unconfined to confined. Groundwater migrates from the southeastern piedmont towards the northwestern valley, subsequently veering westward (Figure 1c). The aquifer exhibits a substantial variability in well yields, with individual wells producing less than 100 m³/d to 5000 m³/d, and as one moves closer to the river valley from both sides of the river, the yield gradually increases. The mid- to high-altitude mountainous strata in the southeastern part of the study area are predominantly composed of Triassic sandstone, and the aquifer type is predominantly characterized as a bedrock fracture system.

Groundwater in the study area primarily originates from the infiltration of atmospheric precipitation and the seasonal melt of snow. Its genesis, occurrence, and distribution are collectively influenced by a suite of interrelated factors. In comparison to surface water, groundwater typically exhibits superior water quality. The higher yields of individual wells and the shallower depth of groundwater in the river valley area facilitate easy extraction of this resource. For the irrigation area, groundwater serves as the principal source of water supply. It is not only indispensable for agricultural and pastoral production but also serves as a vital resource for sustaining the livelihoods of the local population. Consequently, it is essential to assess the water quality of groundwater and comprehend its formation mechanisms to establish a scientific foundation for the conservation of local groundwater resources.

2.2. Water Sampling and Physicochemical Analyses

A total of 27 water samples were collected across the study area in October 2023. Among them, 21 samples are groundwater, while 6 are river water. Among the groundwater samples, four were spring water samples, all of which were collected from the ground surface. The remaining groundwater samples were from phreatic aquifers, with sampling depths ranging from 10 to 30 m. All water samples were evenly distributed throughout the entire study area and had strong representativeness. Except for the spring water samples, all samples were pumped for more than 15 min before collection. The impact of accumulated water in the boreholes/wells on the samples was eliminated. The in situ physicochemical parameters, such as the pH value and electrical conductivity (EC), of the samples were measured on site. The sampling operation was carried out after all in situ physicochemical parameters were stable. The water samples were collected in 500 mL high-density polyethylene bottles after the target water was rinsed 2–3 times. Duplicate sampling was performed at each site to mitigate the risk of potential sampling errors. The samples were sent to the laboratory for hydrochemical analysis within 48 h under a storage temperature of 4 °C.

The on-site measurement device for in situ physicochemical parameters was a portable multi-parameter device (HACH HQ4D, Loveland, CO, USA). The main cations were determined using an inductively coupled plasma mass spectrometer (Agilent 7500ce ICP-MS, Tokyo, Japan). The main anions and NH_4^+ were determined using ion chromatography (Shimadzu LC-10ADVP, Kyoto, Japan). HCO_3^- and TDS were determined using acid–base titration and gravimetric methods, respectively. All samples were tested three times and interspersed with standard controls and blank controls to ensure the accuracy of the test results. The ion charge balance errors of the test results were all within 5, indicating that the test results were reliable.

2.3. Entropy-Weighted Water Quality Index

The entropy-weighted water quality index (EWQI) is an advanced water quality assessment based on the traditional water quality index [45]. This approach introduces the concept of entropy to avoid the influence of human subjectivity to the greatest extent and assigns corresponding weights to each hydrochemical indicator [46,47]. Generally, the evaluation of EWQI goes through the following four steps.

Firstly, the initial eigenvalue matrix **X** for the hydrochemical indicators of water samples is established. The formula for matrix **X** is as follows:

$$X = \begin{bmatrix} x_{11} & x_{12} & \cdots & x_{1n} \\ x_{21} & x_{22} & \cdots & x_{2n} \\ \vdots & \vdots & \ddots & \vdots \\ x_{m1} & x_{m2} & \cdots & x_{mn} \end{bmatrix} \tag{1}$$

where x_{mn} represents the concentration of the nth hydrochemical index of the mth water sample.

Secondly, due to the difference in the dimensions of different hydrochemical indicators, the matrix **X** is normalized to obtain the standardized matrix **Y**. The normalization method and the matrix **Y** are shown in Formulas (2) and (3), respectively.

$$y_{ij} = \frac{x_{ij} - \min(x_{ij})}{\max(x_{ij}) - \min(x_{ij})} \tag{2}$$

$$Y = \begin{bmatrix} y_{11} & y_{12} & \cdots & y_{1n} \\ y_{21} & y_{22} & \cdots & y_{2n} \\ \vdots & \vdots & \ddots & \vdots \\ y_{m1} & y_{m2} & \cdots & y_{mn} \end{bmatrix} \tag{3}$$

where y_{mn} represents the result of normalized x_{mn}.

Next, the entropy weighting method is used to allocate weights to each hydrochemical indicator, which would make the results more formal and objective. The allocation criteria are based on the following formulas:

$$p_{ij} = \frac{y_{ij}}{\sum_{i=1}^{m} y_{ij}} \tag{4}$$

$$e_j = -\frac{1}{\ln m} \sum_{i=1}^{m} p_{ij} \ln(p_{ij}) \tag{5}$$

$$\omega_j = \frac{1 - e_j}{\sum_{j=1}^{n} (1 - e_j)} \tag{6}$$

where p_{ij} represents the proportion of the ith sample in the jth hydrochemical parameter; e_j is the information entropy of each hydrochemical parameter; ω_j represents the entropy weight of each hydrochemical parameter.

Finally, using Formulas (7) and (8), the quantitative grading q_i of each water sample is determined and combined with ω_j to obtain the EWQI of each water sample.

$$q_{ij} = \frac{x_{ij}}{S_j} \times 100 \tag{7}$$

$$EWQI = \sum_{j=1}^{n} \omega_j q_{ij} \tag{8}$$

where x_{ij} is the measured value of the jth hydrochemical parameter of the ith water sample; S_j is the acceptable limit value of the hydrochemical index j recommended by the World Health Organization or Chinese guideline.

2.4. Human Health Risk Assessment

Excessive amounts of a certain toxic ion in drinking water can potentially harm people's health. For different populations, the tolerance to toxic substances usually varies [48]. For non-carcinogenic ions, the health risks of ingestion usually dominate. Therefore, this article focuses on assessing the health risks of oral contact [49].

Firstly, the calculation method for the estimated daily intake (EDI) of toxic elements is based on Formula (9).

$$CDI = \frac{C_i \times IR \times EF \times ED}{BW \times AT} \tag{9}$$

where C_i is the concentration of different toxic ions; IR is the daily water intake; EF and ED represent the exposure frequency and exposure duration, respectively; BW refers to the average weight of different populations; AT is the average time of exposure occurrence.

Afterwards, the non-carcinogenic risk (HQ) for specific toxic substances is calculated using Formula (10).

$$HQ_i = \frac{CDI}{RfD_i} \tag{10}$$

where RfD is the reference value corresponding to the intake dose of a specific pollutant. The overall non-carcinogenic risk (HI) is the sum of the non-carcinogenic risks caused by all toxic substances, and the calculation formula is:

$$HI = \sum_{i=1}^{n} HQ_i \tag{11}$$

2.5. Irrigation Water Quality Assessment

Irrigation water for agriculture is one of the main ways groundwater is consumed in the study area. Unsuitable groundwater can cause crop reduction and even damage soil functions [50]. The assessment of the irrigation adaptability of groundwater has significance for local agricultural development. The irrigation water quality index (IWQI) can objectively evaluate the quality of agricultural water through multiple parameters [51]. For this research, considering the actual situation of the study area, the sodium adsorption ratio (SAR), soluble sodium percentage (%Na), and permeability index (PI) are selected to evaluate the irrigation adaptability of groundwater [52].

SAR measures the cation exchange that occurs in the soil due to irrigation water. It reflects the degree of Na^+ adsorption in the soil. The larger the SAR value, the higher the Na^+ content in the soil and the stronger the soil alkalization [53]. The calculation for SAR is shown in Formula (12).

$$SAR = \frac{Na^+}{\sqrt{\frac{Mg^{2+}+Ca^{2+}}{2}}} \times 100\% \tag{12}$$

%Na is an important indicator reflecting the potential Na hazard in irrigation water. It reflects the proportion of Na^+ in the cations of irrigation water. Higher Na^+ can damage soil structure and reduce its permeability [49]. The calculation for %Na is shown in Formula (13).

$$\%Na = \frac{Na^+ + K^+}{Na^+ + K^+ + Mg^{2+} + Ca^{2+}} \times 100\% \tag{13}$$

PI is another important indicator reflecting irrigation adaptability. It is used to reflect the impact of Na^+, HCO_3^-, Ca^{2+}, and Mg^{2+} in irrigation water on soil permeability. The calculation for PI is shown in Formula (14).

$$PI = \frac{Na^+ + \sqrt{HCO_3^-}}{Ca^{2+} + Mg^{2+} + Na^+} \times 100\% \tag{14}$$

3. Results and Discussion

3.1. General Hydrochemical Characteristics

To preliminarily realize the overall hydrochemical characteristics of surface water and groundwater in the study area, the physicochemical data of collected river waters and groundwaters are summarily presented in Tables 1 and 2. The corresponding drinking guidelines of various indexes recommended by the Chinese Guideline [54] and World Health Organization [55] are also included in the Tables for comparison.

The pH value of collected river waters was 7.76–7.97 with a mean of 7.85, and that of collected groundwaters was 7.07–8.06 with an average of 7.70. Both river water and groundwater in the study area had pH values slightly greater than 7, demonstrating a neutral to a little alkaline nature. River water and groundwater TDS was in the range of 297.39–368.57 mg/L (averaging 328.90 mg/L) and 300.25–638.38 mg/L (averaging 399.86 mg/L), respectively. Notably, groundwater had a higher TDS value than river water

in the study area, although both had relatively low TDS. This may be related to the relatively long residence time of groundwater in the aquifer, which could provide more than enough time for groundwater to react with the deposits. Both the slightly alkaline nature and the very fresh characteristic of river water and groundwater imply that water in the study area—regardless if it is above or beneath the ground surface—has relatively good quality and keeps a natural, or approximately natural, status.

Table 1. Summary of river water physicochemical indexes in the study area and corresponding drinking water standard.

Index	Unit	Min	Max	Mean	SD *	Guideline	% of the Sample Exceeding the Guideline
pH	/	7.76	7.97	7.85	0.09	6.5–8.5 **	0%
TDS	mg/L	297.39	368.57	328.90	27.47	1000 **	0%
K^+	mg/L	2.07	2.49	2.26	0.21	/	
Na^+	mg/L	9.41	36.05	22.54	8.95	200 **	0%
Ca^{2+}	mg/L	38.08	102.20	71.48	24.82	75 ***	50%
Mg^{2+}	mg/L	9.72	46.17	21.67	14.93	50 ***	0%
Cl^-	mg/L	10.64	39.00	18.91	10.44	250 **	0%
SO_4^{2-}	mg/L	14.41	57.64	36.02	18.91	250 **	0%
HCO_3^-	mg/L	262.39	341.71	302.05	30.81	/	
NO_3^-	mg/L	8.46	17.23	12.58	3.85	50.0 ***	0%
NO_2^-	mg/L	0.00	0.00	0.00	0.00	0.02 **	0%
NH_4^+	mg/L	0.08	0.24	0.16	0.08	0.2 **	33.33%

* Standard deviation; ** Chinese Guideline [54]; *** WHO Guideline [55].

Table 2. Summary of groundwater physicochemical indexes in the study area and corresponding drinking water standard.

Index	Unit	Min	Max	Mean	SD *	Guideline	% of the Sample Exceeding the Guideline
pH	/	7.07	8.06	7.70	0.25	6.5–8.5 **	0%
TDS	mg/L	300.25	638.38	399.86	90.01	1000 **	0%
K^+	mg/L	0.56	54.36	5.99	11.55	/	
Na^+	mg/L	7.62	117.10	40.28	29.30	200 **	0%
Ca^{2+}	mg/L	48.1	112.22	76.82	21.28	75 ***	42.86%
Mg^{2+}	mg/L	8.51	49.82	22.68	10.73	50 ***	0%
Cl^-	mg/L	10.64	106.35	35.28	28.44	250 **	0%
SO_4^{2-}	mg/L	9.61	220.94	44.83	44.73	250 **	0%
HCO_3^-	mg/L	250.18	524.77	336.77	62.99	/	
NO_3^-	mg/L	3.58	42.86	16.09	8.80	50.0 ***	0%
NO_2^-	mg/L	0.00	0.08	0.01	0.02	0.02 **	9.09%
NH_4^+	mg/L	0.06	1.42	0.22	0.29	0.2 **	28.57%

* Standard deviation; ** Chinese Guideline [54]; *** WHO Guideline [55].

Among the major cations, Ca^{2+} is the predominant ion for river water, with a concentration in the range of 38.08–102.20 mg/L, followed by Mg^{2+}, Na^+, and K^+. The sampled river water in the study area had Mg^{2+}, Na^+, and K^+ concentrations in the ranges of 9.72–46.17 mg/L, 9.41–36.05 mg/L, and 2.07–2.49 mg/L, respectively. The concentration of major anions in river water was in the order of $HCO_3^- > SO_4^{2-} > Cl^-$; the concentration of HCO_3^- (262.39–341.71 mg/L) is far greater than that of SO_4^{2-} (14.41–57.64 mg/L) and Cl^- (10.64–39.00 mg/L). Ca^{2+} is the predominant ion among the major cations of groundwater and ranges from 48.10 mg/L to 112.22 mg/L (mean of 76.82 mg/L). The second most predominant cation for groundwater is distinct from river water. Na^+ ranks second among the major cations of groundwater, with the concentration varying between 7.62 mg/L and 117.10 mg/L (mean of 40.28 mg/L). Mg^{2+} and K^+ rank third and fourth among the major cations of groundwater, respectively, with concentrations in the ranges of

8.51–49.82 mg/L (mean of 22.68 mg/L) and 0.56–54.36 mg/L (mean of 5.99 mg/L). The major anions of groundwater present the same concentration order as river water, i.e., $HCO_3^- > SO_4^{2-} > Cl^-$. The collected groundwaters in the study area have a HCO_3^- concentration ranging from 250.18 mg/L to 524.77 mg/L. SO_4^{2-} concentration varies from 9.61 to 220.94 mg/L, with a mean of 44.83 mg/L. Cl^- is in the range of 10.64–106.35 mg/L, with an average of 35.28 mg/L. All the major ions (including cations and anions) of river water and groundwater were within the drinking water standards except Ca^{2+} (Tables 1 and 2). About 50.00% and 42.86% of sampled river waters and groundwaters were above the standard of 75 mg/L recommended by WHO for drinking purposes [55]. However, they only slightly exceeded the recommended drinking standard of Ca^{2+}.

Nitrogen contaminants (including NO_3^-, NO_2^-, NH_4^+) were also detected in this research. The concentrations of NO_3^- were in the range of 8.46–17.23 mg/L for river water and 3.58–42.86 mg/L for groundwater, respectively, with a mean of 12.58 mg/L and 16.09 mg/L. All sampled waters—regardless of whether they were above or below the ground surface—were within the NO_3^- the drinking standard concentration recommended by WHO (below 50 mg/L) [55]. The concentration of NO_2^- was very low for river water and within the drinking standard of 0.02 mg/L given by the Chinese Guideline [54]. Groundwater in the study area had higher NO_2^- concentrations than river water, with a maximum of 0.08 mg/L. Approximately 9.09% of the collected groundwater samples had NO_2^- concentrations beyond the drinking standard of 0.02 mg/L. The concentration of NH_4^+ varied from 0.08 mg/L to 0.24 mg/L, with an average of 0.16 mg/L for river water and between 0.06 mg/L and 1.42 mg/L, with an average of 0.22 mg/L for groundwater. Both river water and groundwater had NH_4^+ contents exceeding the recommendations by the Chinese Guideline [54] in some sampling locations (accounting for 33.33% and 28.57% of sampling sites for river water and groundwater, respectively).

3.2. Hydrochemical Types

The hydrochemical types of surface (river) water and groundwater in the present study area were visually identified based on the Piper trilinear diagram. The Piper trilinear diagram is composed of three sub-diagrams, including two triangles below and one diamond above. The two triangles below were used to demonstrate the major cation ($Na^+ + K^+$, Mg^{2+}, Ca^{2+}) and ion (Cl^-, SO_4^{2-}, HCO_3^-) compositions, respectively. The diamond above is used to synthetically illustrate the hydrochemical types of water.

As demonstrated in Figure 2, the collected river waters dominantly plotted in A and B of the left triangle, demonstrating that Ca^{2+} was the predominant cation, followed by Mg^{2+}. For groundwater, it can be seen that although most of the collected groundwater samples were situated in A, many present a distributing trend towards C dominance, with some directly plotting in C. Some sporadic groundwater samples were situated in the boundary area of B dominance. All of the above suggests that Ca^{2+} is an overwhelmingly dominant cation in the unconfined aqueous environment, followed by Na^{2+} and Mg^{2+}. This is consistent with the above cation orders based on the average concentration. Overall, the surface water and groundwater in the study area were mainly characterized as [Ca^{2+}] type.

For anions, it can be seen that all collected river water samples were situated in the left corner of D. dominance in the right triangle (Figure 2), implying that river water in the study area is dominated by HCO_3^-. Groundwater samples were also all situated in D, suggesting that HCO_3^- is the predominant anion for groundwater. Notably, groundwater samples also showed a trend from the left corner to the upper and right direction of D, indicating that the groundwater is much saltier than river water. As a whole, river water and groundwater in the study area were characterized as [HCO_3^-] type.

For the synthetical chemical feature, all river waters were situated in the left corner of dominance 1 of the diamond, indicating that river waters in the study area are very fresh in nature. The collected groundwaters were also dominantly in the 1 of the diamond but showed a distributing trend from the left corner to the right direction with one even in the 3. This indicates that groundwater has saltier hydrochemical features than river

water. Overall, river waters were characterized by hydrochemical type HCO_3-Ca, and groundwaters were hydrochemical type HCO_3-Ca and HCO_3-Na·Ca.
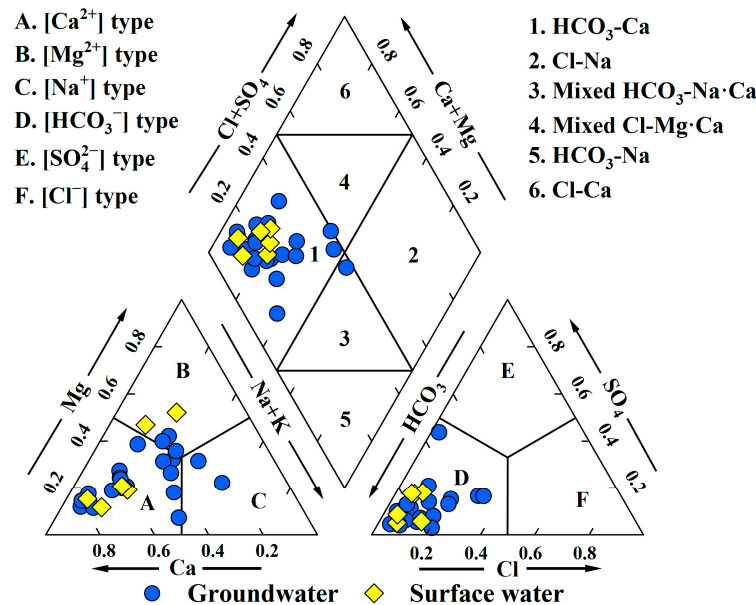

Figure 2. Piper diagram illustrating the hydrochemical composition of river water and groundwater in the study area.

3.3. Formation of Groundwater Chemistry

Natural factors form the basis of the hydrochemical composition of groundwater. In general, the major natural mechanisms potentially governing the hydrochemical composition of groundwater are precipitation, rock–water interactions, and evaporation [56]. "Precipitation" represents the hydrochemical feature of recharge water, which is usually atmospheric water. "Rock–water interactions" signifies all the processes that occur between aquifer media and groundwater from the moment water infiltrates the aquifer until it is extracted or moves on. "Evaporation" refers to the evaporation effects on groundwater, primarily affecting phreatic groundwater that is located at shallow depths. These three major natural mechanisms can be revealed by the relationship of the $Na^+/(Na^++Ca^{2+})$ ratio versus TDS and $Cl^-/(Cl^-+HCO_3^-)$ versus the TDS ratio [57].

As depicted in Figure 3, all groundwater samples collected from the phreatic aquifers plotted in the rock dominance, indicating that the hydrochemical composition of phreatic groundwater is predominantly controlled by rock–water interactions in nature. No groundwater samples situated in the precipitation dominance, implying that no sampled phreatic groundwater retained the hydrochemical composition of recharge water. This is because the groundwater flows very slowly, giving it enough time to react with the aquifer media. In addition, the collected phreatic groundwaters were not in the evaporation dominance, suggesting that evaporation effects are also not significant to the hydrochemical composition of phreatic groundwater in the study area.

To further reveal the specifics of the rock–water interaction, the relationships between the Ca^{2+}/Na^+ ratio and Mg^{2+}/Na^+ ratio and between the Ca^{2+}/Na^+ ratio and HCO_3^-/Na^+ ratio were explored. Three major rock/mineral types can be identified by these two relations, including carbonates, silicates, and evaporites. As demonstrated in Figure 4, the collected phreatic groundwater samples were dominantly situated in or around the silicate dominance, indicating that silicate weathering (Formula (15)) is the dominant process contributing to the chemical constituents of phreatic groundwater in the study area. Meanwhile, phreatic groundwater in some sporadic sites is also observed distributing towards the evaporite and carbonate dominance, suggesting that the dissolution of evaporites and carbonates can also contribute chemical constituents to groundwater to some degree.
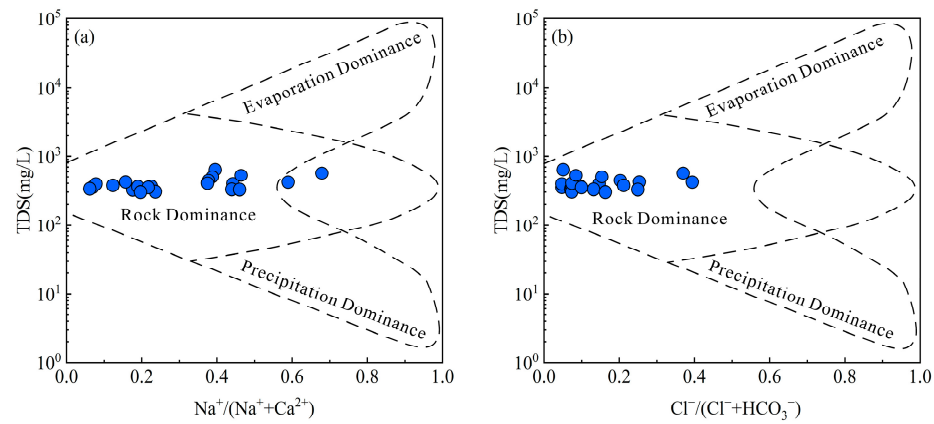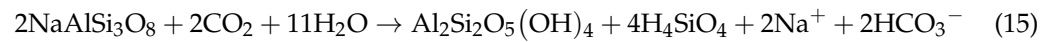
$$2NaAlSi_3O_8 + 2CO_2 + 11H_2O \rightarrow Al_2Si_2O_5(OH)_4 + 4H_4SiO_4 + 2Na^+ + 2HCO_3^- \quad (15)$$

Figure 3. Gibbs diagram of (**a**) $Na^+/(Na^++Ca^{2+})$ versus TDS and (**b**) $Cl^-/(Cl^-+HCO_3^-)$ versus TDS for the sampled groundwaters in the study area.
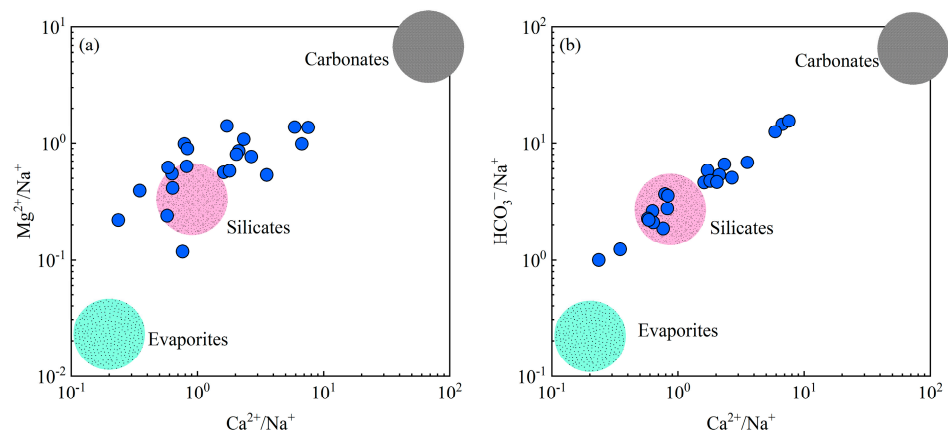

Figure 4. End-member diagram of (**a**) Ca^{2+}/Na^+ versus Mg^{2+}/Na^+ and (**b**) Ca^{2+}/Na^+ versus HCO_3^-/Na^+ illustrating the minerals contributing to groundwater chemistry.

Besides the aforementioned rock weathering and mineral dissolution, ion exchange is also a non-negligible process that occurs in the aquifer, particularly in fine sedimentary aquifers. The chlor-alkali index (CA1-1 and CAI-2) is introduced to gain insights into potential ion exchange processes, which can be calculated by Formulas (16) and (17). As shown in Figure 5a, most of the collected samples have negative values for both CA1-1 and CAI-2, implying the occurrence of the cation-exchange reaction (Formula (18)) in the aquifer. Meanwhile, three samples had positive values for both CA1-1 and CAI-2, indicating existing reverse cation-exchange reactions (Formula (19)) in the aquifer of these sporadic sites. The relation between $(Na^++K^+-Cl^-)$ and $(Ca^{2+}+Mg^{2+}-HCO_3^--SO_4^{2-})$ is also introduced to verify these ion exchange processes. As depicted in Figure 5b, it is confirmed that the cation-exchange reaction is the dominant ion-exchange process in the phreatic aquifers, and the reverse cation-exchange reaction also occurred at some sporadic sites.

$$CAI - 1 = \frac{Cl^- - (Na^+ + K^+)}{Cl^-} \quad (16)$$

$$CAI - 2 = \frac{Cl^- - (Na^+ + K^+)}{HCO_3^- + SO_4^{2-} + CO_3^{2-} + NO_3^-} \quad (17)$$

$$2\text{Na}^+ + \text{CaX}_2 \text{ (or MgX}_2\text{) (solids)} \rightarrow \text{Ca}^{2+}\left(\text{or Mg}^{2+}\right) + 2\text{NaX (solids)} \tag{18}$$

$$\text{Ca}^{2+}\left(\text{or Mg}^{2+}\right) + 2\text{NaX (solids)} \rightarrow 2\text{Na}^+ + \text{CaX}_2 \text{ (or MgX}_2\text{) (solids)} \tag{19}$$
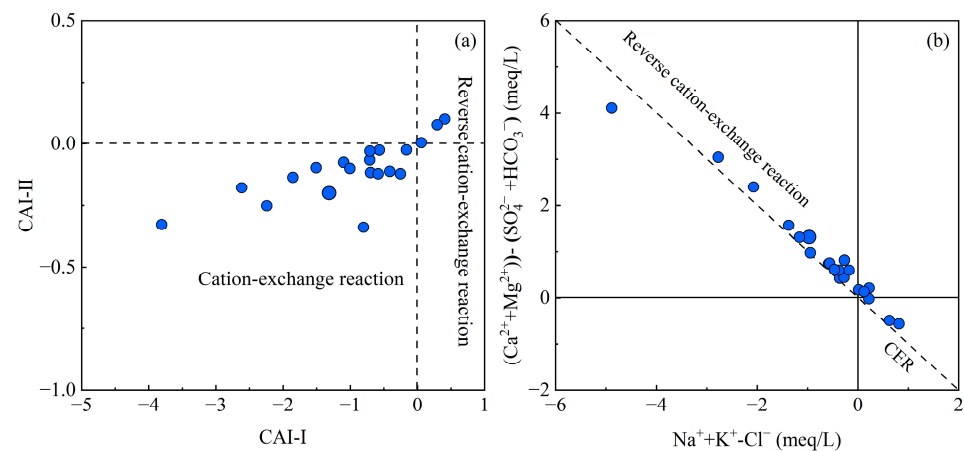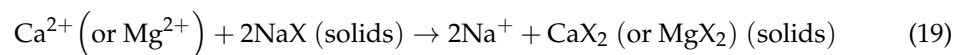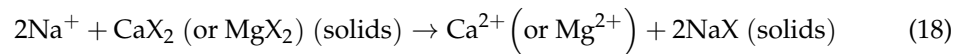

Figure 5. Scatter plots of (**a**) CAI-I versus CAI-II and (**b**) ($\text{Na}^+ + \text{K}^+ - \text{Cl}^-$) versus ($\text{Ca}^{2+} + \text{Mg}^{2+} - \text{HCO}_3^- - \text{SO}_4^{2-}$) of groundwater in the study area. RCER defines the reverse cation-exchange reaction; CER denotes the cation-exchange reaction.

Although all sampled groundwater had NO_3^- concentrations below the drinking standard of 50 mg/L recommended by WHO [55], most groundwater samples exceeded the geological background limit of 10 mg/L [58] (Figure 6a). This implies that phreatic groundwater in the study area has been influenced by human activities in its hydrochemical composition, especially nitrite. The relation of the Cl^-/Na^+ ratio versus $\text{NO}_3^-/\text{Na}^+$ ratio was employed to gain insights into the specific source of the nitrate pollutant. As depicted in Figure 6b, the sampled groundwaters dominantly plotted adjacent to agricultural activities, implying that NO_3^- in phreatic groundwater primarily originates from agricultural practices. It can be concluded that agricultural practices have led to widespread inputs of nitrogen pollutants to phreatic aquifers, although the level of pollution is still relatively low.
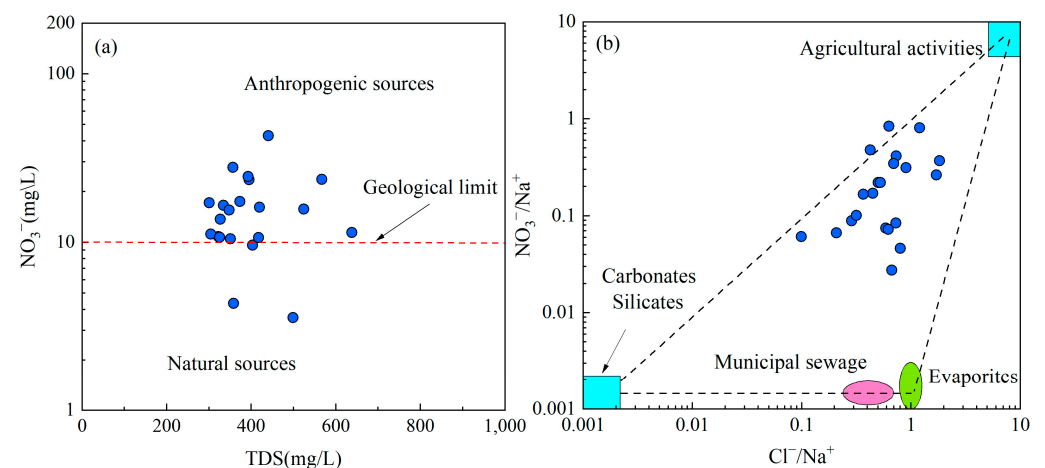

Figure 6. Scatter plots of (**a**) TDS versus NO_3^- and (**b**) Cl^-/Na^+ versus $\text{NO}_3^-/\text{Na}^+$ of groundwater in the study area.

The Pearson correlation coefficients are introduced to gain insights into the influence of agricultural practices on groundwater chemical composition besides NO_3^-. As shown in Table 1, the groundwater at some sampling sites had a relatively high content of NH_4^+, and approximately 33.33% of samples exceeded the permissible limit recommended by the Chinese Guideline [54]. Considering the potential contamination sources in the study area,

these exceeding NH_4^+ contaminants originated from chemical fertilizers of agricultural practices. In addition, some hydrochemical indicators such as Cl^-, Na^+, K^+, and TDS presented a positive relation with NH_4^+ (Figure 7), indicating that agricultural practices also brought chemical solutes into phreatic groundwaters, especially Cl^-, Na^+, and K^+. Although agricultural practices introduce some solutes (including nitrogen contaminants and chemical solutes) and increase the salinity of groundwater, to some extent, the perturbations are relatively limited for the overall framework of groundwater hydrochemistry (Figure 7).
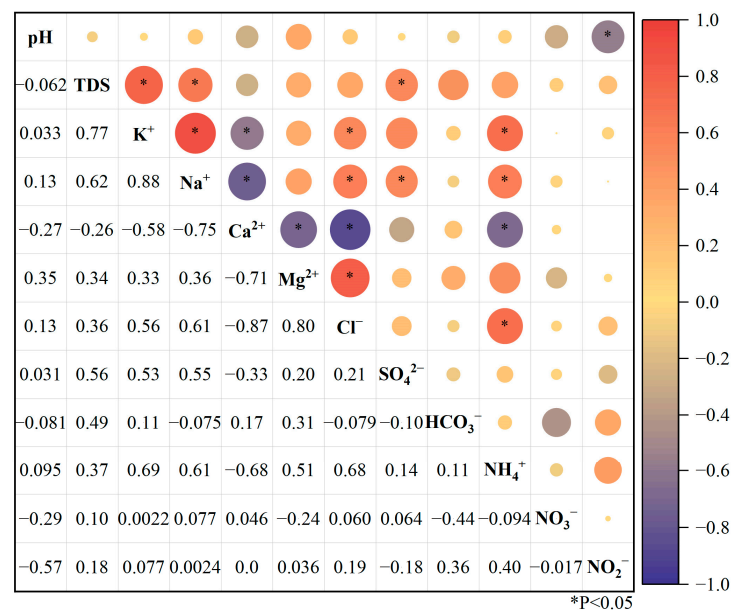
pH											
−0.062	TDS										
0.033	0.77	K^+									
0.13	0.62	0.88	Na^+								
−0.27	−0.26	−0.58	−0.75	Ca^{2+}							
0.35	0.34	0.33	0.36	−0.71	Mg^{2+}						
0.13	0.36	0.56	0.61	−0.87	0.80	Cl^-					
0.031	0.56	0.53	0.55	−0.33	0.20	0.21	SO_4^{2-}				
−0.081	0.49	0.11	−0.075	0.17	0.31	−0.079	−0.10	HCO_3^-			
0.095	0.37	0.69	0.61	−0.68	0.51	0.68	0.14	0.11	NH_4^+		
−0.29	0.10	0.0022	0.077	0.046	−0.24	0.060	0.064	−0.44	−0.094	NO_3^-	
−0.57	0.18	0.077	0.0024	0.0	0.036	0.19	−0.18	0.36	0.40	−0.017	NO_2^-

*$P < 0.05$

Figure 7. Correlation of various hydrochemical parameters and their correlation coefficients for groundwater in the study area.

3.4. Groundwater Quality Evaluation

3.4.1. Drinking Water Quality

Groundwater is widely used as drinking water in alpine areas like the present study area. The chemical quality suitability of groundwater for drinking purposes was evaluated using the EWQI approach. The results show that the phreatic groundwater in the study area had a relatively large range of EWQI values from 25.7 to 159.9 (Figure 8), suggesting that phreatic groundwater in the present area has a wide variation of hydrochemical quality. As demonstrated in Figure 8, most of the collected phreatic groundwater samples (95.24%) had EWQI values below 100, suggesting it is suitable for direct drinking purposes. Particularly, about 80.95% of the sampled groundwaters had EWQI values below 50, belonging to the excellent water quality rank (rank 1). Only one groundwater sample (4.76%) had an EWQI value beyond 100 and reached 159.88, which is characterized by a poor water quality rank (rank 4). Phreatic groundwater in this sampling site (G09) should be avoided for direct drinking. The main reason for the poor quality of phreatic groundwater at sampling site G09 is the relatively high content of NH_4^+, originating from agricultural activities.

In addition to the overall quality revealed by the EWQI assessment, the potential health hazards of toxic substances, including NH_4^+, NO_2^-, and NO_3^-, were assessed using the HHRA model. The HQ values of NH_4^+ and NO_2^- in phreatic groundwater were all below 1 for all sampling sites (Figure 9a,b), implying that these two nitrogen pollutants would not pose significant health hazards to water consumers through the oral pathway. Meanwhile, the HQ values of NO_{3-} showed a relatively large variation for all population groups. The HQ_{NO3} values range from 0.08 to 1.02 for adult males, between 0.09 and 1.08 for adult females, from 0.09 to 1.10 for children, and between 0.16 and 1.87 for infants (Figure 9c). Only one sampling site (G10) had HQ_{NO3} values exceeding the permissible

limit of 1 for adult male, adult female, and children, with maximum values of 1.02, 1.08, and 1.10, respectively. Four sampling sites were identified with HQ_{NO3} values exceeding the permissible limit of 1 in infants, G01, G06, G10, and G11, with respective HQ_{NO3} values of 1.03, 1.08, 1.87, and 1.22.
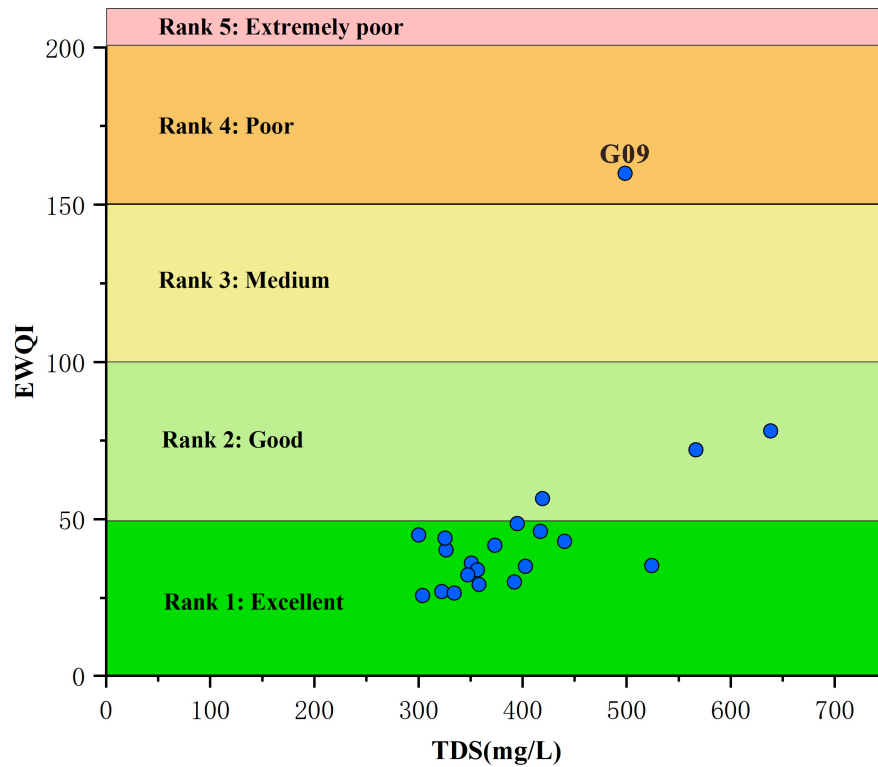

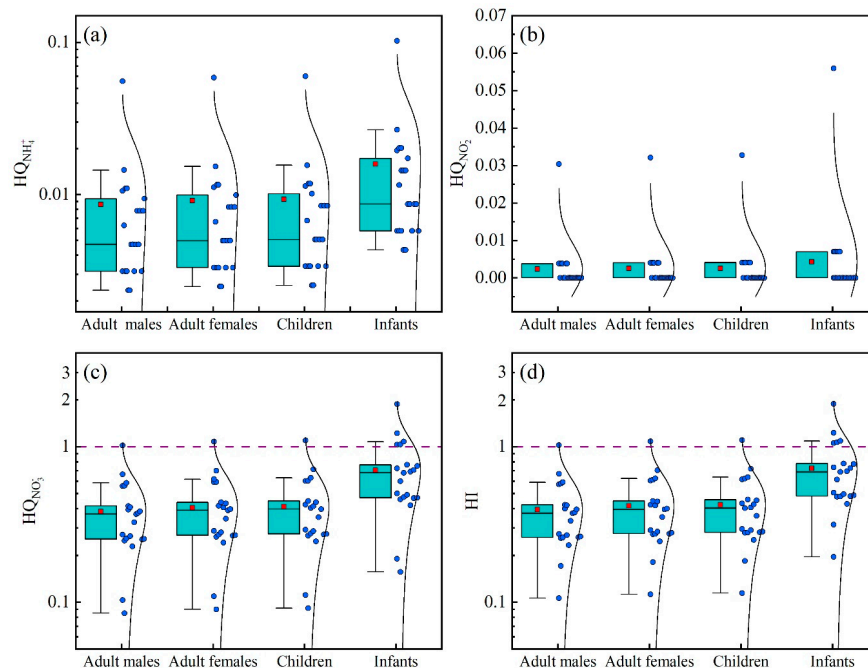**Figure 8.** Scatter plots of TDS versus EWQI of groundwater in the study area.

Figure 9. Box plots of HQ values of (**a**) NH_4^+, (**b**) NO_2^-, (**c**) NO_3^-, and (**d**) HI values of groundwater in the study area.

The HI values are in the range of 0.11–1.02 for adult males, 0.11–1.08 for adult females, 0.11–1.10 for children, and 0.20–1.88 for infants, with an average of 0.39, 0.42, 0.42, and 0.72, respectively (Figure 9d). Approximately 4.76%, 4.76%, 4.76%, and 19.05% of collected groundwater samples had HI values beyond the permissible limit of 1 for the aforementioned four population groups, indicating potential health risk. As discussed above, the HQ values of NH_4^+ and NO_2^- for all populations were very small, while those of NO_3^- were larger in variation. Thus, the overall health risks are primarily posed by the nitrate pollutant phreatic in groundwater. However, phreatic groundwaters at most sampling sites had HI values below the safe limit of 1, indicating a low and negligible risk. The only groundwater sample (G10) with potential health risks for adult males and females (HI value just slightly beyond the permissible limit of 1) had values of 1.02 and 1.08, respectively. This suggests that the potential health risk of groundwater at sampling site G10 is very limited for adults. Although four sampling sites had HI values exceeding the permissible limit of 1 for infants, two were just slightly beyond 1. Only two sampling sites had relatively large HI values, with 1.88 for G10 and 1.23 for G11. For children, the only sampling site with a potential health risk was with an HI value of 1.10. Therefore, approximately 4.76% (1 sampling site, G10) and 9.52% (2 sampling sites, G10 and G11) had slightly significant health risks for water consumption in children and infants, respectively.

3.4.2. Irrigation Water Quality

Groundwater, especially in the phreatic aquifers, is primarily utilized for agricultural irrigation in alpine areas. The suitability of water quality for irrigation depends on the content of hydrochemical ions in water and how they affect the soils and plants [59]. EC is a comprehensive parameter demonstrating the overall content of chemical ions in water. Generally, water with EC values less than 250 μS/cm and in the range of 250–750 μS/cm is regarded as excellent and good quality, respectively, and suitable for irrigation. Water with EC values in the range of 750–2250 μS/cm is considered a doubtful quality for irrigation, and that beyond 2250 μS/cm is unsuitable for irrigation. As demonstrated in Table 3, the EC values of phreatic groundwater samples vary from 509.73 μS/cm to 944.06 μS/cm, averaging at 670.22 μS/cm. Approximately 76.19% of sampled phreatic groundwaters had EC values in the range of 250–750 μS/cm, implying they are good for irrigation. Meanwhile, about 23.81% of the samples had EC values in the range of 750-2250 μS/cm, belonging to the doubtful quality category.

Table 3. Assessment results of groundwater quality for irrigation in the study area.

Index	Unit	Range	Class	Percentage
EC	μS/cm	<250	Excellent	/
		250–750	Good	76.19%
		750–2250	Doubtful	23.81%
		>2250	Unsuitable	/
SAR	meq/L	<10	Excellent	100%
		10–8	Good	/
		18–26	Doubtful	/
		>26	Unsuitable	/
%Na	%	<20	Excellent	52.38%
		20–40	Good	38.10%
		40–60	Permissible	9.52%
		60–80	Doubtful	/
		>80	Unsuitable	/
PI	%	<25	Unsuitable	/
		25–75	Moderately suitable	95.24%
		>75	Suitable	4.76%

The excessive Na^+ in irrigation water compared with ions of Mg^{2+} and Ca^{2+} would damage the permeability of the soil, which can be assessed by the SAR. The calculated results show that the SAR values of sampled phreatic groundwaters in the study area range between 0.19 and 3.34 and are all below 10, indicating excellent quality (Table 3). The Wilcox diagram is introduced to assess the potential overall hazards for agricultural irrigation. It can be seen from Figure 10 that about 76.19% and 23.81% of the collected phreatic groundwater samples belong to the C2S1 and C3S1 categories, respectively, indicating medium and high salinity hazards but a low sodium hazard for all. It can be seen that most of the study area has groundwater of medium salinity hazard and low sodium hazard (C2S1) rather than high salinity hazard and low sodium hazard (C3S1) (Figure 11a). Groundwaters with high salinity hazards and low sodium hazards (C3S1) are scattered throughout the research area (Figure 11a).
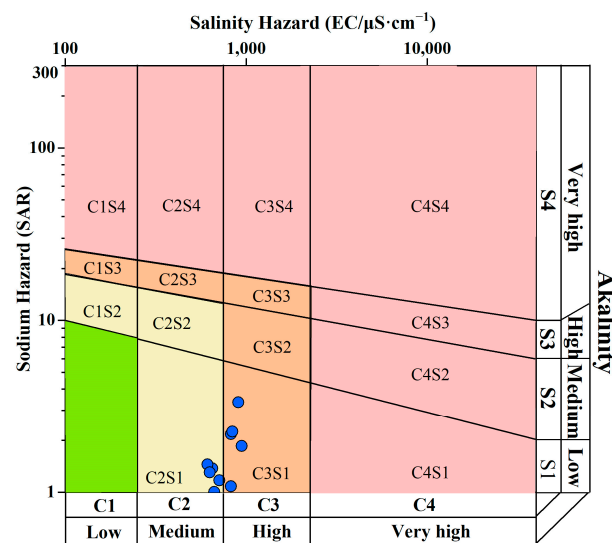

Figure 10. Wilcox diagram demonstrating irrigation quality of groundwater in the study area.
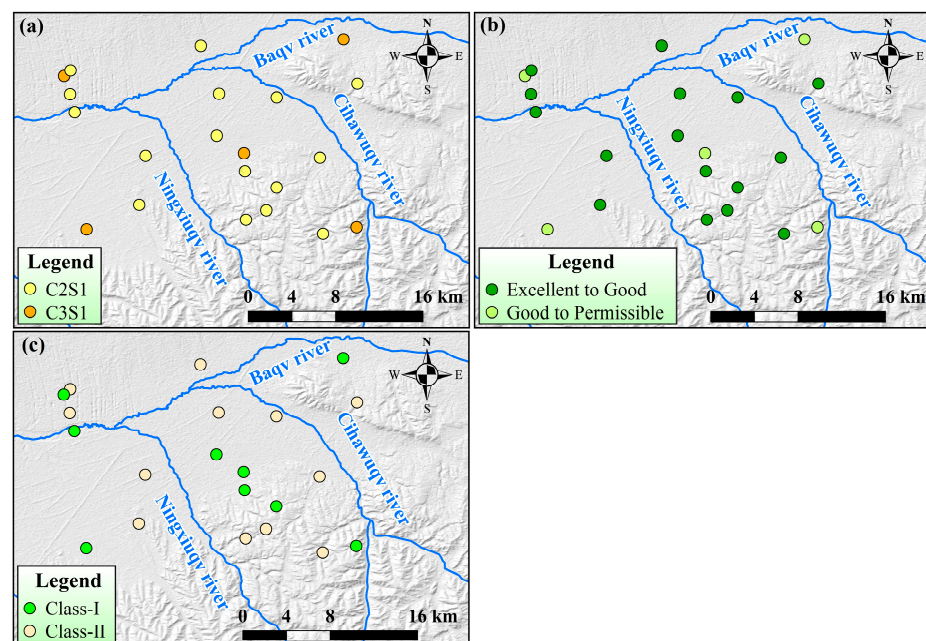

Figure 11. Spatial distribution of groundwater quality for irrigation demonstrated by (**a**) Wilcox diagram classification, (**b**) USSL diagram classification, and (**c**) Doneen diagram classification.

The %Na was further used to assess the potential effect of Na⁺ on soil permeability. As seen in the calculated results, it ranges from 5.26 to 50.76, with a mean of 21.47. It can be seen from Table 3 that about 52.38% of the samples are divided into the excellent quality category for irrigation in terms of %Na. Approximately 38.10% and 9.52% of the groundwater samples belong to the good and permissible irrigation quality, respectively. In addition, the USSL diagram, which considers the EC and %Na at the same time, is introduced to evaluate the integrated irrigation quality of phreatic groundwater. As shown in Figure 12, the majority (76.19%) of collected groundwater samples are situated in the category of excellent to good quality, and the rest of the samples (23.81%) belong to the category of good to permissible quality. Thus, all phreatic groundwaters are suitable for irrigation in terms of the %Na. The distribution of groundwater quality classified by the USSL diagram (Figure 11b) is similar to that classified by the Wilcox diagram (Figure 11a). Most of the study area's groundwater quality is excellent to good. Groundwaters with good to permissible quality are scattered throughout the research area (Figure 11b).
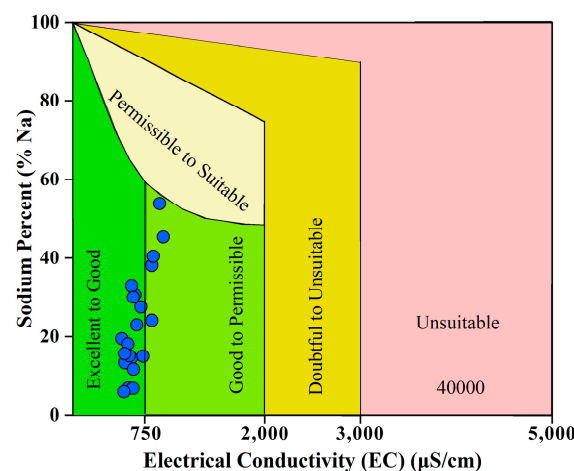

Figure 12. USSL diagram contracted by the relation between EC and sodium percent of groundwater in the study area.

The PI value is employed to gain insights into the potential effects of dissolved chemical ions in irrigation water on soil. The calculated PI values are in the range of 39.51–75.59, with a mean of 53.82. Approximately 95.24% and 4.76% of phreatic groundwater samples belong to the moderately suitable and suitable categories for irrigation in terms of PI assessment results (Table 3). An integrated diagram constructed by PI and the total concentration of chemical ions is employed. As depicted in Figure 13, about 42.86% of sampled groundwaters are situated in the Class-I category, indicating good quality for irrigation in terms of permeability. Other samples (57.14%) belong to the Class-II category, demonstrating suitable quality for irrigation purposes. Thus, there is no potential threat to soil permeability when using phreatic groundwater for irrigation in terms of the assessment of PI. Groundwaters that have the irrigation quality of Class-I are mainly distributed away from the river channel, and groundwaters adjacent to rivers are irrigation quality Class-II (Figure 11c).

Overall, phreatic groundwater in the study area is of relatively good quality for irrigation purposes and would not pose a sodium hazard or cause potential permeability damage to soil. Although groundwater at most sampling sites (76.19%) is suitable for irrigation, a small portion of sampling sites (23.81%) have a potential salinity hazard for the phreatic groundwater and should be considered during the long-term sustainable irrigation practice.
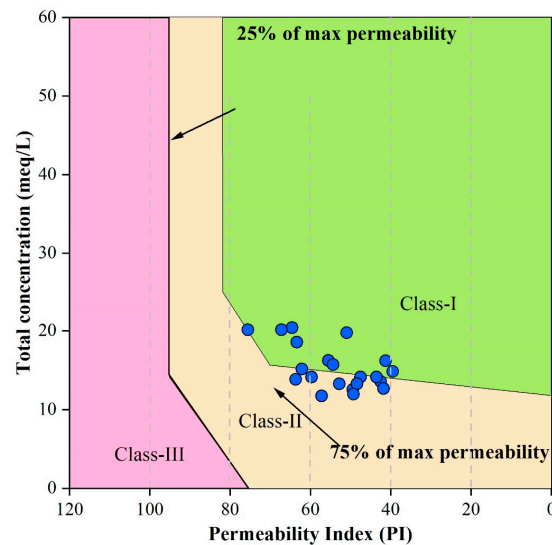
Figure 13. Doneen diagram illustrating the relation between permeability index and total concentration of groundwater in the study area.

3.5. Implication for Sustainable Development of Groundwater Resources in Alpine Regions

Groundwater in alpine regions is significant for the local development and the water circulation of the hydrosphere as it is in the headwater region. At the same time, it is vulnerable to external disturbances, including global climate change and human activities. Generally, groundwater in the alpine regions is of a natural status, which is usually of good quality. However, with the strengthening of human activities and the intensification of climate change, groundwater resources are facing unprecedented challenges. The present research takes a typical irrigation alpine region of the Tibetan Plateau to gain insights into the hydrochemical status, quality, and formation of groundwater in alpine regions with dense human irrigation practices.

Phreatic groundwater in present irrigation alpine regions retains the natural, slightly alkaline, and fresh features but is slightly saltier than recharged river water. All forms of nitrogen contaminants (NO_3^-, NO_2^-, and NH_4^+) had higher concentrations in phreatic groundwater than in river water and originated from agricultural practices like chemical fertilizer application. This demonstrates that phreatic groundwater in the present alpine plain has deteriorated by agricultural practices [60,61]. Thus, agricultural contaminants should be considered and managed. It is recommended to transition from chemical fertilizers to organic alternatives, such as animal manure, for their eco-friendly benefits and sustainable environmental development.

Groundwater quality has been influenced by the aforementioned agricultural nitrogen contaminants and their availability for direct drinking usage at some sporadic sites (G09). The relatively high content of NO_3^- would potentially threaten the health of local humans, especially for minors. Groundwater serves as a viable resource for sustainable long-term irrigation without adversely affecting soil permeability. However, the potential for salinization at some sites must be carefully managed to ensure the sustainability of agricultural practices if groundwater is used for long-term irrigation. As global climate change and human activities escalate, it is anticipated that groundwater resources in alpine regions will be increasingly threatened by pollution and are at risk of natural degradation, such as salinization. Thus, more attention should be paid to the groundwater resources of these headwater regions.

4. Conclusions

The Tibetan Plateau is the "Third Pole" of the earth and the "Asia Water Tower", and its alpine regions are sensitive and fragile to changes in the external environment. Groundwater resources are essential for the sustainable development of alpine regions

on the Tibetan Plateau. The present research takes a typical area on the Tibetan Plateau to obtain insights into the hydrochemistry and suitability of phreatic groundwater for sustainable usage in the alpine agricultural area. The main findings are below.

Phreatic groundwater keeps a slightly alkaline and fresh nature in the present alpine irrigation area with a pH varying from 7.07 to 8.06 and TDS in the range of 300.25–638.38 mg/L, which is very similar to the hydrochemical features of river water but slightly saltier. Groundwater is characterized by a hydrochemical type of HCO_3-Ca and HCO_3-Na·Ca. This composition is also slightly more variable compared to that of river water, which typically exhibits a HCO_3-Ca type. The majority of major ions are in relatively low concentrations and within the desirable limit for drinking purposes, except for Ca^{2+}. All forms of nitrogen contaminants have higher concentrations in phreatic groundwater than in river water. All phreatic groundwaters have NO_3^- content in the range of 3.58–42.86 mg/L with a mean of 16.09 mg/L, which are all within the drinking standard of 50 mg/L. The maximum concentration of NO_2^- and NH_4^+ in groundwater reaches 0.08 mg/L and 1.42 mg/L, respectively. Approximately 9.09% and 28.57% of collected groundwaters are beyond the permissible limit of NO_2^- (0.02 mg/L) and NH_4^+ (0.2 mg/L) for drinking purposes.

Groundwater has relatively good hydrochemical quality for domestic usage based on the entropy-weighted water quality index assessment. Although the EWQI value of phreatic groundwater is in a large range of 25.7 to 159.9, most groundwaters (95.24%) have an EWQI value below 100 and are suitable for direct drinking. At one of the sampling sites, designated as G09, the EWQI exceeds 100, reaching up to 159.9. This high value indicates that the water is classified within the poor water quality category and ascribed to the relatively high content of NH_4^+ (1.42 mg/L). The high concentration of NO_3^- in groundwater would potentially threaten the health of minors at some sporadic sites in the study area, with a maximum HI value of 1.88 for infants and 1.10 for children. The SAR and %Na value of phreatic groundwater vary between 0.19 and 3.34 and from 5.26 to 50.76, respectively. The Na^+ content in groundwater is acceptable for irrigation and would not damage the soil permeability. The PI value of groundwater ranges from 39.51 to 75.59 and also presents no threat to the soil permeability. While the EC value of groundwater has a relatively large variation from 250–750 μS/cm, 23.81% of collected groundwaters had doubtful quality for irrigation and may pose a potential salinity hazard during long-term irrigation practices.

The hydrochemical composition of groundwater is primarily governed by rock–water interactions rather than the original recharge water (precipitation) and evaporation. Silicate weathering is the predominant process that contributes dissolved chemicals to groundwater. The dissolution of evaporites and carbonates can also contribute some chemical constituents to phreatic groundwater but to a very limited degree. The cation-exchange reaction is the dominant ion-exchange process in phreatic aquifers and influences the hydrochemical composition of groundwater in most sampling sites. Reverse cation-exchange reactions also occur in the aquifer but only at some sporadic sites. Agricultural practice has resulted in the elevation of nitrogen contaminants, which are dominant in the form of NO_3^- and NH_4^+ rather than NO_2^-. The major chemicals are not significantly brought into the phreatic groundwater during this process. It is crucial to address agricultural nitrogen pollutants to safeguard invaluable groundwater resources and foster the sustainable development of these water assets in alpine irrigation regions.

Author Contributions: S.Y.: field investigation, methodology, formal analysis, writing–original draft; Z.Z.: conceptualization, formal analysis, writing–reviewing and editing; S.W.: conceptualization, formal analysis; S.X.: field investigation, formal analysis; Y.X.: conceptualization, formal analysis, writing—reviewing and editing; J.W. (Jie Wang): field investigation, data curation, methodology, formal analysis; J.W. (Jianhui Wang): field investigation, methodology, formal analysis; Y.Y.: formal analysis, data curation, methodology; R.B.: formal analysis, data curation, methodology; N.W.: methodology, writing–reviewing and editing; Y.Z.: field investigation, methodology, formal analysis; L.W.: methodology, data curation, formal analysis; H.Y.: field investigation, formal analysis. All authors have read and agreed to the published version of the manuscript.

Data Availability Statement: The data used to support the findings of the present study will be provided upon request by the corresponding author.

Conflicts of Interest: Authors Shaokang Yang, Zhen Zhao, Shengbin Wang, Shanhu Xiao, Jianhui Wang, Youjin Yuan and Ruishou Ba were employed by Qinghai 906 Engineering Survey and Design Institute Co., Ltd. The remaining authors declare that the research was conducted in the absence of any commercial or financial relationships that could be construed as a potential conflict of interest.

References

1. Immerzeel, W.W.; Lutz, A.F.; Andrade, M.; Bahl, A.; Biemans, H.; Bolch, T.; Hyde, S.; Brumby, S.; Davies, B.J.; Elmore, A.C.; et al. Importance and vulnerability of the world's water towers. *Nature* **2020**, *577*, 364–369. [CrossRef] [PubMed]
2. Crawford, J.T.; Hinckley, E.-L.S.; Litaor, M.I.; Brahney, J.; Neff, J.C. Evidence for accelerated weathering and sulfate export in high alpine environments. *Environ. Res. Lett.* **2019**, *14*, 124092. [CrossRef]
3. Xiao, Y.; Zhang, Y.; Yang, H.; Wang, L.; Han, J.; Hao, Q.; Wang, J.; Zhao, Z.; Hu, W.; Wang, S.; et al. Interaction regimes of surface water and groundwater in a hyper-arid endorheic watershed on Tibetan Plateau: Insights from multi-proxy data. *J. Hydrol.* **2024**, *644*, 132020. [CrossRef]
4. Viviroli, D.; Kummu, M.; Meybeck, M.; Kallio, M.; Wada, Y. Increasing dependence of lowland populations on mountain water resources. *Nat. Sustain.* **2020**, *3*, 917–928. [CrossRef]
5. Tian, L.; Guo, S.; Feng, J.; He, C. Quantifying the altitudinal response of water yield capacity to climate change in an alpine basin on the Tibetan Plateau through integrating the WRF-Hydro and Budyko framework. *CATENA* **2024**, *242*, 108087. [CrossRef]
6. Halloran, L.J.S.; Millwater, J.; Hunkeler, D.; Arnoux, M. Climate change impacts on groundwater discharge-dependent streamflow in an alpine headwater catchment. *Sci. Total Environ.* **2023**, *902*, 166009. [CrossRef]
7. Xu, N.; Lu, H.; Li, W.Y.; Gong, P. Natural lakes dominate global water storage variability. *Sci. Bull.* **2024**, *69*, 1016–1019. [CrossRef]
8. Guo, X.; Feng, Q.; Yin, Z.; Si, J.; Xi, H.; Zhao, Y. Critical role of groundwater discharge in sustaining streamflow in a glaciated alpine watershed, northeastern Tibetan Plateau. *Sci. Total Environ.* **2022**, *822*, 153578. [CrossRef]
9. Schädler, B.; Weingartner, R. Impact of Climate Change on Water Resources in the Alpine Regions of Switzerland. In *Alpine Waters*; Bundi, U., Ed.; Springer: Berlin/Heidelberg, Germany, 2010; pp. 59–69. [CrossRef]
10. Xiao, Y.; Liu, K.; Hao, Q.; Xiao, D.; Zhu, Y.; Yin, S.; Zhang, Y. Hydrogeochemical insights into the signatures, genesis and sustainable perspective of nitrate enriched groundwater in the piedmont of Hutuo watershed, China. *Catena* **2022**, *212*, 106020. [CrossRef]
11. He, Q.; Kuang, X.; Ma, E.; Chen, J.; Feng, Y.; Zheng, C. Evolution of runoff components and groundwater discharge under rapid climate warming: Lhasa river basin, Tibetan Plateau. *J. Hydrol.* **2024**, *628*, 130556. [CrossRef]
12. Evans, S.G.; Ge, S.; Voss, C.I.; Molotch, N.P. The Role of Frozen Soil in Groundwater Discharge Predictions for Warming Alpine Watersheds. *Water Resour. Res.* **2018**, *54*, 1599–1615. [CrossRef]
13. Somers, L.D.; McKenzie, J.M.; Mark, B.G.; Lagos, P.; Ng, G.-H.C.; Wickert, A.D.; Yarleque, C.; Baraër, M.; Silva, Y. Groundwater Buffers Decreasing Glacier Melt in an Andean Watershed—But Not Forever. *Geophys. Res. Lett.* **2019**, *46*, 13016–13026. [CrossRef]
14. Meng, Y.; Liu, G.; Li, M. Tracing the Sources and Processes of Groundwater in an Alpine Glacierized Region in Southwest China: Evidence from Environmental Isotopes. *Water* **2015**, *7*, 2673–2690. [CrossRef]
15. Shen, H.; Rao, W.; Tan, H.; Guo, H.; Ta, W.; Zhang, X. Controlling factors and health risks of groundwater chemistry in a typical alpine watershed based on machine learning methods. *Sci. Total Environ.* **2023**, *854*, 158737. [CrossRef] [PubMed]
16. Peña Reyes, F.A.; Crosta, G.B.; Frattini, P.; Basiricò, S.; Della Pergola, R. Hydrogeochemical overview and natural arsenic occurrence in groundwater from alpine springs (upper Valtellina, Northern Italy). *J. Hydrol.* **2015**, *529*, 1530–1549. [CrossRef]
17. Giménez-Forcada, E.; Luque-Espinar, J.A.; López-Bahut, M.T.; Grima-Olmedo, J.; Jiménez-Sánchez, J.; Ontiveros-Beltranena, C.; Díaz-Muñoz, J.Á.; Elster, D.; Skopljak, F.; Voutchkova, D.; et al. Analysis of the geological control on the spatial distribution of potentially toxic concentrations of As and F- in groundwater on a Pan-European scale. *Ecotoxicol. Environ. Saf.* **2022**, *247*, 114161. [CrossRef]
18. Gomez, L.; Alvarez, A.; D'Ambrosio, S.; Zalazar, G.; Aravena, R. Use of isotopes techniques to reveal the origin of water salinity in an arid region of Central-Western Argentina. *Sci. Total Environ.* **2021**, *763*, 142935. [CrossRef]
19. Qu, S.; Zhao, Y.; Zhang, K.; Wang, J.; Li, M.; Yang, X.; Ren, X.; Hao, Y.; Yu, R. Multi-isotopes (δD, $\delta 18Owater$, $87Sr/86Sr$, $\delta 34S$ and $\delta 18Osulfate$) as indicators for groundwater salinization genesis and evolution of a large agricultural drainage lake basin in Inner Mongolia, Northwest China. *Sci. Total Environ.* **2024**, *946*, 174181. [CrossRef]

20. Zhao, Y.; Zhang, Y.; Yan, Y.; Wen, Y.; Zhang, D. Geographic distribution and impacts of climate change on the suitable habitats of two alpine Rhododendron in Southwest China. *Glob. Ecol. Conserv.* **2024**, *54*, e03176. [CrossRef]

21. Kumar, S.; Chatterjee, U.; David Raj, A.; Sooryamol, K.R. Global Warming and Climate Crisis/Extreme Events. In *Climate Crisis: Adaptive Approaches and Sustainability*; Chatterjee, U., Shaw, R., Kumar, S., Raj, A.D., Das, S., Eds.; Springer Nature: Cham, Switzerland, 2023; pp. 3–18. [CrossRef]

22. Fu, C.-c.; Li, X.-q.; Cheng, X. Unraveling the mechanisms underlying lake expansion from 2001 to 2020 and its impact on the ecological environment in a typical alpine basin on the Tibetan Plateau. *China Geol.* **2023**, *6*, 216–227. [CrossRef]

23. Liu, Y.; Wei, L.; Huang, A.; Peng, B.; Shu, Q. Spatial and temporal evolution of soil water and its response to the environment in the Yangtze River source area under climate change. *Hydrogeol. Eng. Geol.* **2023**, *50*, 39–52.

24. Vörösmarty, C.J.; Green, P.; Salisbury, J.; Lammers, R.B. Global water resources:: Vulnerability from climate change and population growth. *Science* **2000**, *289*, 284–288. [CrossRef] [PubMed]

25. Wang, Z.; Cao, S.; Cao, G.; Hou, Y.; Wang, Y.; Kang, L. Implications for water management in alpine inland river basins: Evidence from stable isotopes and remote sensing. *Ecol. Indic.* **2023**, *154*, 110580. [CrossRef]

26. Zhang, Q.; Shen, Z.; Pokhrel, Y.; Farinotti, D.; Singh, V.P.; Xu, C.-Y.; Wu, W.; Wang, G. Oceanic climate changes threaten the sustainability of Asia's water tower. *Nature* **2023**, *615*, 87–93. [CrossRef]

27. Qin, Y.; Jin, X.; Jin, Y.; Mao, X.; Du, K. Simulation and prediction of runoff in cold alpine basins under climate change conditions. *J. Salt Lake Res.* **2024**, *32*, 29–38.

28. Han, F.; Liu, T.; Huang, Y.; Zan, C.; Pan, X.; Xu, Z. Response of water quality to climate warming and atmospheric deposition in an alpine lake of Tianshan Mountains, Central Asia. *Ecol. Indic.* **2023**, *147*, 109949. [CrossRef]

29. Yi, B.; Liu, J.; He, W.; Lu, X.; Cao, X.; Chen, X.; Zeng, X.; Zhang, Y. Optical variations of dissolved organic matter due to surface water-groundwater interaction in alpine and arid Datonghe watershed. *Sci. Total Environ.* **2023**, *864*, 161036. [CrossRef] [PubMed]

30. Ronchetti, F.; Deiana, M.; Lugli, S.; Sabattini, M.; Critelli, V.; Aguzzoli, A.; Mussi, M. Water isotope analyses and flow measurements for understanding the stream and meteoric recharge contributions to the Poiano evaporite karst spring in the North Apennines, Italy. *Hydrogeol. J.* **2023**, *31*, 601–619. [CrossRef]

31. Kumar, R.; Saika, M.; Vishwakarma, D.K.; Al-Ansari, N.; Nand Lal, K.; Elbeltagi, A.; Kallem, S.; Prasad, V.; Kuriqi, A. Assessment of Climate Change Impact on Snowmelt Runoff in Himalayan Region. *Sustainability* **2022**, *14*, 1150. [CrossRef]

32. Singh, R.; Kayastha, S.P.; Shrestha, S.M.; Sapkota, R.P. Hydro-geochemical conditions under projected climate change scenarios of Marshyangdi River, Nepal. *Theor. Appl. Climatol.* **2024**, *155*, 5375–5387. [CrossRef]

33. Fida, M.; Li, P.; Wang, Y.; Alam, S.M.K.; Nsabimana, A. Water Contamination and Human Health Risks in Pakistan: A Review. *Expo. Health* **2023**, *15*, 619–639. [CrossRef]

34. Taucare, M.; Viguier, B.; Figueroa, R.; Daniele, L. The alarming state of Central Chile's groundwater resources: A paradigmatic case of a lasting overexploitation. *Sci. Total Environ.* **2024**, *906*, 167723. [CrossRef] [PubMed]

35. Wang, M.; Su, C.; Wang, X.; Jiang, J.; Ren, F.; Liu, H. Spatial pattern, hydrogeochemical controlling processes and non-carcinogenic risks of fluoride-enriched groundwater in the North Henan Plain, Northern China. *Appl. Geochem.* **2024**, *163*, 105934. [CrossRef]

36. Deiana, M.; Mussi, M.; Pennisi, M.; Boccolari, M.; Corsini, A.; Ronchetti, F. Contribution of water geochemistry and isotopes ($\delta18O$, $\delta2H$, 3H, 87Sr/86Sr and $\delta11B$) to the study of groundwater flow properties and underlying bedrock structures of a deep landslide. *Environ. Earth Sci.* **2019**, *79*, 30. [CrossRef]

37. Morin-Crini, N.; Lichtfouse, E.; Liu, G.; Balaram, V.; Ribeiro, A.R.L.; Lu, Z.; Stock, F.; Carmona, E.; Teixeira, M.R.; Picos-Corrales, L.A.; et al. Worldwide cases of water pollution by emerging contaminants: A review. *Environ. Chem. Lett.* **2022**, *20*, 2311–2338. [CrossRef]

38. Richards, L.A.; Kumari, R.; White, D.; Parashar, N.; Kumar, A.; Ghosh, A.; Kumar, S.; Chakravorty, B.; Lu, C.; Civil, W.; et al. Emerging organic contaminants in groundwater under a rapidly developing city (Patna) in northern India dominated by high concentrations of lifestyle chemicals. *Environ. Pollut.* **2021**, *268*, 115765. [CrossRef]

39. Qu, S.; Duan, L.; Shi, Z.; Mao, H.; Wang, G.; Liu, T.; Yu, R.; Peng, X. Identifying the spatial pattern, driving factors and potential human health risks of nitrate and fluoride enriched groundwater of Ordos Basin, Northwest China. *J. Clean. Prod.* **2022**, *376*, 134289. [CrossRef]

40. Deléglise, C.; François, H.; Loucougaray, G.; Crouzat, E. Facing drought: Exposure, vulnerability and adaptation options of extensive livestock systems in the French Pre-Alps. *Clim. Risk Manag.* **2023**, *42*, 100568. [CrossRef]

41. Gugulothu, S.; Subbarao, N.; Das, R.; Dhakate, R. Geochemical evaluation of groundwater and suitability of groundwater quality for irrigation purpose in an agricultural region of South India. *Appl. Water Sci.* **2022**, *12*, 142. [CrossRef]

42. Alam, S.M.K.; Li, P.; Fida, M. Groundwater Nitrate Pollution Due to Excessive Use of N-Fertilizers in Rural Areas of Bangladesh: Pollution Status, Health Risk, Source Contribution, and Future Impacts. *Expo. Health* **2024**, *16*, 159–182. [CrossRef]

43. Jiang, W.; Meng, L.; Liu, F.; Sheng, Y.; Chen, S.; Yang, J.; Mao, H.; Zhang, J.; Zhang, Z.; Ning, H. Distribution, source investigation, and risk assessment of topsoil heavy metals in areas with intensive anthropogenic activities using the positive matrix factorization (PMF) model coupled with self-organizing map (SOM). *Environ. Geochem. Health* **2023**, *45*, 6353–6370. [CrossRef] [PubMed]

44. Ma, W.; Wu, T.; Wu, X.; Yang, S.; Li, R.; Zhou, S.; Li, X.; Zhu, X.; Hao, J.; Ni, J.; et al. Carbon budgets and environmental controls in alpine ecosystems on the Qinghai-Tibet Plateau. *Catena* **2023**, *229*, 107224. [CrossRef]

45. Abidi, J.H.; Elzain, H.E.; Sabarathinam, C.; Selmane, T.; Selvam, S.; Farhat, B.; Ben Mammou, A.; Senapathi, V. Evaluation of groundwater quality indices using multi-criteria decision-making techniques and a fuzzy logic model in an irrigated area. *Groundw. Sustain. Dev.* **2024**, *25*, 101122. [CrossRef]

46. Siddique, M.; Islam, A.; Hasanuzzaman, M.; Khan, R.; Akbor, M.A.; Hossain, M.; Sajid, M.; Mia, M.; Mallick, J.; Rahman, M.; et al. Multivariate statistics and entropy theory for irrigation water quality and entropy-weighted index development in a subtropical urban river, Bangladesh. *Environ. Sci. Pollut. Res.* **2022**, *29*, 8577–8596. [CrossRef]

47. Rahman, M.A.; Siddique, M.A.B.; Khan, R.; Reza, A.H.M.S.; Khan, A.H.A.N.; Akbor, M.A.; Islam, M.S.; Hasan, A.B.; Hasan, M.I.; Elius, I.B. Mechanism of arsenic enrichment and mobilization in groundwater from southeastern Bangladesh: Water quality and preliminary health risks assessment. *Chemosphere* **2022**, *294*, 133556. [CrossRef]

48. Haji, M.; Karuppannan, S.; Qin, D.; Shube, H.; Kawo, N.S. Potential Human Health Risks Due to Groundwater Fluoride Contamination: A Case Study Using Multi-techniques Approaches (GWQI, FPI, GIS, HHRA) in Bilate River Basin of Southern Main Ethiopian Rift, Ethiopia. *Arch. Environ. Contam. Toxicol.* **2021**, *80*, 277–293. [CrossRef]

49. Chen, F.; Yao, L.; Mei, G.; Shang, Y.; Xiong, F.; Ding, Z. Groundwater Quality and Potential Human Health Risk Assessment for Drinking and Irrigation Purposes: A Case Study in the Semiarid Region of North China. *Water* **2021**, *13*, 783. [CrossRef]

50. Khan, S.; Ullah, Q.; Khan, A.A.; Hassan, S.S.; Shakoor, A.; Ijaz, M. Geostatistical investigation of groundwater quality zones for its applications in irrigated agriculture areas of Punjab (Pakistan). *Environ. Earth Sci.* **2022**, *81*, 91. [CrossRef]

51. Li, R.; Yan, Y.; Xu, J.; Yang, C.; Chen, S.; Wang, Y.; Zhang, Y. Evaluate the groundwater quality and human health risks for sustainable drinking and irrigation purposes in mountainous region of Chongqing, Southwest China. *J. Contam. Hydrol.* **2024**, *264*, 104344. [CrossRef] [PubMed]

52. Mukate, S.; Wagh, V.; Panaskar, D.; Jacobs, J.A.; Sawant, A. Development of new integrated water quality index (IWQI) model to evaluate the drinking suitability of water. *Ecol. Indic.* **2019**, *101*, 348–354. [CrossRef]

53. Benaafi, M.; Pradipta, A.; Tawabini, B.; Al-Areeq, A.M.; Bafaqeer, A.; Humphrey, J.D.; Nazal, M.K.; Aljundi, I.H. Suitability of treated wastewater for irrigation and its impact on groundwater resources in arid coastal regions: Insights for water resources sustainability. *Heliyon* **2024**, *10*, e29320. [CrossRef] [PubMed]

54. *GB/T 14848-2017*; Standards for Groundwater Quality. General Administration of Quality Supervision: Beijing, China, 2017.

55. WHO. *Guidelines for Drinking-Water Quality*, 4th ed.; Incorporating the First Addendum; World Health Organization: Geneva, Switzerland, 2017.

56. Zhang, Y.; Xiao, Y.; Yang, H.; Wang, S.; Wang, L.; Qi, Z.; Han, J.; Hao, Q.; Hu, W.; Wang, J. Hydrogeochemical and isotopic insights into the genesis and mixing behaviors of geothermal water in a faults-controlled geothermal field on Tibetan Plateau. *J. Clean. Prod.* **2024**, *442*, 140980. [CrossRef]

57. Gibbs, R.J. Mechanisms controlling world water chemistry. *Science* **1970**, *170*, 1088–1090. [CrossRef] [PubMed]

58. Xiao, Y.; Hao, Q.; Zhang, Y.; Zhu, Y.; Yin, S.; Qin, L.; Li, X. Investigating sources, driving forces and potential health risks of nitrate and fluoride in groundwater of a typical alluvial fan plain. *Sci. Total Environ.* **2022**, *802*, 149909. [CrossRef]

59. Francis, V.; Krishnaraj, S.; Kumar, S.; Andiyappan, R.K.; Govindan, P. GIS-based groundwater potential zonation and assessment of groundwater quality and suitability for drinking and irrigation purposes in the Shanmughanadhi river basin, south India. *Kuwait J. Sci.* **2024**, *51*, 100243. [CrossRef]

60. Han, R.; Liu, W.; Zhang, J.; Zhao, T.; Sun, H.; Xu, Z. Hydrogeochemical characteristics and recharge sources identification based on isotopic tracing of alpine rivers in the Tibetan Plateau. *Environ. Res.* **2023**, *229*, 115981. [CrossRef]

61. Kang, X.B.; Xu, M.; Li, K.; Liu, X. Exploration and utilisation of groundwater resources in extreme arid regions of the Tibetan Plateau: A case study on Ali area, China. *J. Earth Syst. Sci.* **2020**, *129*, 208. [CrossRef]